Journal of Chemistry

Synthesis of Boron-Based Compounds and Nanostructures for Biomedical Applications

Lead Guest Editor: Pervaiz Ahmad
Guest Editors: Israf Ud Din and Jibran Iqbal

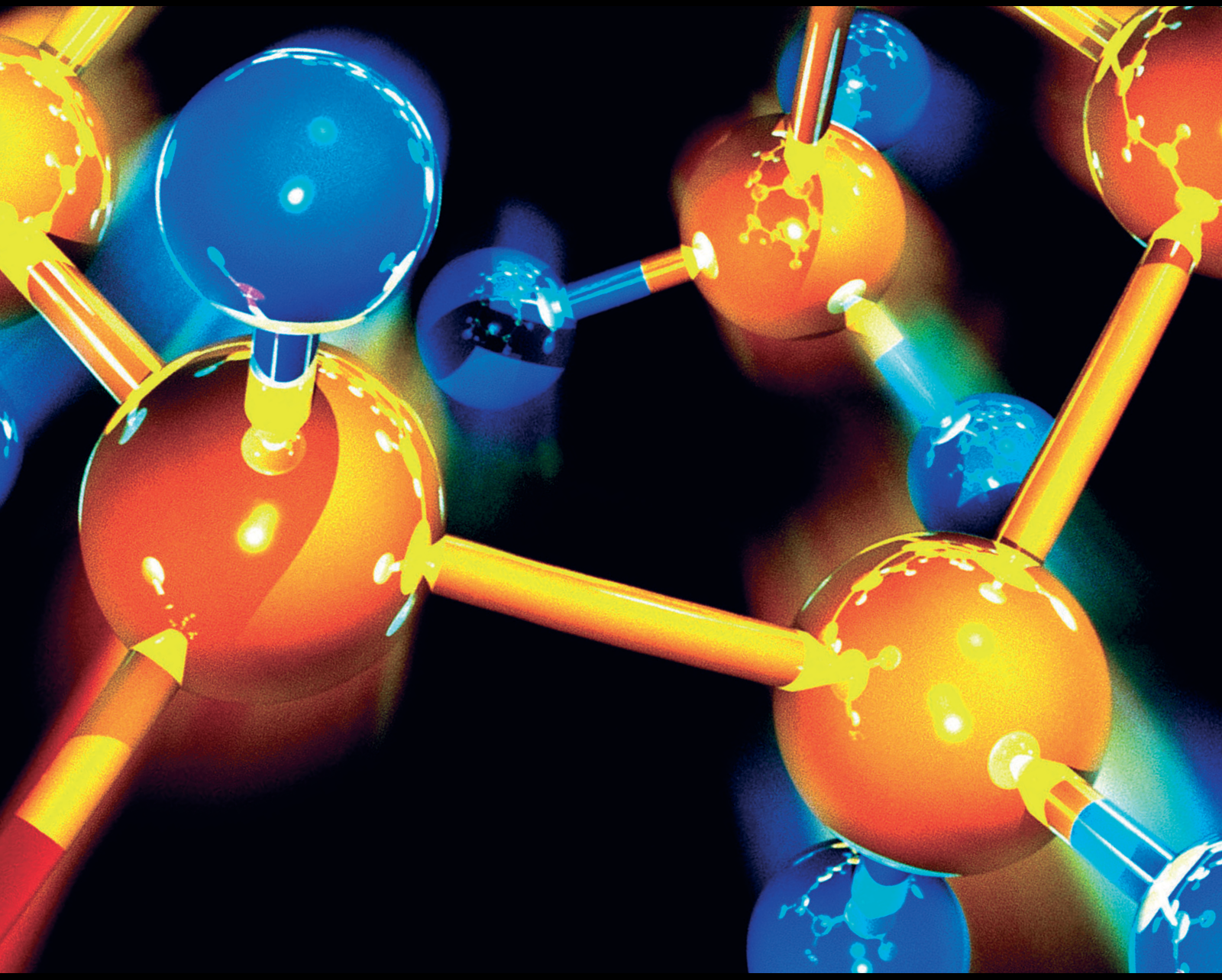

Synthesis of Boron-Based Compounds and Nanostructures for Biomedical Applications

Journal of Chemistry

Synthesis of Boron-Based Compounds and Nanostructures for Biomedical Applications

Lead Guest Editor: Pervaiz Ahmad
Guest Editors: Israf Ud Din and Jibran Iqbal

Chief Editor

Kaustubha Mohanty, India

Associate Editors

Mohammad Al-Ghouti, Qatar
Tingyue Gu, USA
Teodorico C. Ramalho, Brazil
Artur M. S. Silva, Portugal

Academic Editors

Jinwei Duan , China
Luqman C. Abdullah, Malaysia
Dr Abhilash, India
Amitava Adhikary, USA
Amitava Adhikary, USA
Mozhgan Afshari, Iran
Daryoush Afzali, Iran
Mahmood Ahmed, Pakistan
Islam Al-Akraa, Egypt
Juan D. Alché, Spain
Gomaa A. M. Ali, Egypt
Mohd Sajid Ali, Saudi Arabia
Shafaqat Ali, Pakistan
Patricia E. Allegretti, Argentina
Marco Anni, Italy
Alessandro Arcovito, Italy
Hassan Arida, Saudi Arabia
Umair Ashraf, Pakistan
Narcis Avarvari, France
Davut Avci, Turkey
Chandra Azad, USA
Mohamed Azaroual, France
Rasha Azzam, Egypt
Hassan Azzazy, Egypt
Renal Backov, France
Suresh Kannan Balasingam, Republic of Korea
Sukanta Bar, USA
Florent Barbault, France
Maurizio Barbieri, Italy
James Barker, United Kingdom
Salvatore Barreca, Italy
Jorge Barros-Velázquez, Spain
THANGAGIRI Baskaran, India
Haci Baykara, Ecuador
Michele Benedetti, Italy
Laurent Billon, France
Marek Biziuk, Poland
Jean-Luc Blin, France
Tomislav Bolanca, Croatia
Ankur Bordoloi, India
Cato Brede, Norway
Leonid Breydo, USA
Wybren J. Buma, The Netherlands
J. O. Caceres, Spain
Patrizia Calaminici, Mexico
Claudio Cameselle, Spain
Joaquin Campos, Spain
Dapeng Cao, China
Domenica Capasso, Italy
Stefano Caporali, Italy
Zenilda Cardeal, Brazil
Angela Cardinali, Italy
Stefano Carli, Italy
Maria F. Carvalho, Portugal
Susana Casal, Portugal
David E. Chavez, USA
Riccardo Chelli, Italy
Zhongfang Chen, Puerto Rico
Vladislav Chrastny, Czech Republic
Roberto Comparelli, Italy
Filomena Conforti, Italy
Luca Conti, Italy
Christophe Coquelet, France
Filomena Corbo, Italy
Jose Corchado, Spain
Maria N. D.S. Cordeiro, Portugal
Claudia Crestini, Italy
Gerald Culioli, France
Nguyen Duc Cuong, Vietnam
Stefano D'Errico, Italy
Matthias D'hooghe, Belgium
Samuel B. Dampare, Ghana
Umashankar Das, Canada
Victor David, Romania
Annalisa De Girolamo, Italy
Antonio De Lucas-Consuegra, Spain
Marcone A. L. De Oliveira, Brazil
Paula G. De Pinho, Portugal
Damião De Sousa, Brazil
Francisco Javier Deive, Spain
Tianlong Deng, China

Contents

Hindawi
Journal of Chemistry
Volume 2023, Article ID 4574604, 12 pages
https://doi.org/10.1155/2023/4574604

Research Article

First-Principle Studies of the Structural, Electronic, and Optical Properties of Double-Walled Carbon Boron Nitride Nanostructures Heterosystem under Various Interwall Distances

Yahaya Saadu Itas,[1] Abdussalam Balarabe Suleiman,[2] Chifu E. Ndikilar,[2] Abdullahi Lawal,[3] Razif Razali,[4] Ismail Ibrahim Idowu,[2] Mayeen Uddin Khandaker,[5,6] Amina Muhammad Danmadami,[1] Pervaiz Ahmad,[7] Talha Bin Emran,[8] and Mohammad Rashed Iqbal Faruque[9]

[1]*Department of Physics, Bauchi State University Gadau, PMB 65, Gadau, Bauchi, Nigeria*
[2]*Department of Physics, Federal University, Dutse, Nigeria*
[3]*Department of Physics, Federal College of Education, Zaria, Nigeria*
[4]*Department of Physics Faculty of Science, Universiti Teknologi, Johor Bahru, Malaysia*
[5]*Department of General Educational Development, Faculty of Science and Information Technology, Daffodil International University, DIU Rd, Dhaka 1341, Bangladesh*
[6]*Centre for Applied Physics and Radiation Technologies, School of Engineering and Technology, Sunway University, Bandar Sunway 47500, Selangor, Malaysia*
[7]*Department of Physics, University of Azad Jammu and Kashmir, Muzaffarabad 13100, Pakistan*
[8]*Department of Pharmacy, BGC Trust University Bangladesh, Chittagong 4381, Bangladesh*
[9]*Space Science Centre, Institute of Climate Change, Universiti Kebangsaan Malaysia, Bangi 43600, Selangor DE, Malaysia*

Correspondence should be addressed to Mayeen Uddin Khandaker; mayeenk@diu.edu.bd

Received 4 November 2022; Revised 17 December 2022; Accepted 18 March 2023; Published 7 April 2023

Academic Editor: Ashanul Haque

Structural, electronic, and optical properties of a new combined system of carbon and boron nitride nanotubes are studied using the DFT first principles as implemented in Quantum ESPRESSO codes. The corrections to the quasi-particle energies were studied via GW hybrid functional implemented in the YAMBO code within the many-body perturbation theory. The studies were performed under different interwall distances of 3.0 nm, 2.5 nm, and 1.5 nm between CNTs and BNNTs. The results showed that the structural properties demonstrated high stability of the double-walled carbon boron nitride nanotube (DWCBNNT) systems under interwall distance (IWD) of 3.00 nm, 2.50 nm, and 1.50 nm. Results also demonstrated an inverse variation between the IWD and the diameter of the DWCBNNT system. In terms of the electronic properties, all three configurations of the DWCBNNTs reveal semiconducting behavior under KS-DFT showing a direct band gap of 3.30 eV, 1.79 eV, and 0.81 eV under IWD of 3.0 nm, 2.5 nm, and 1.5 nm, respectively. Furthermore, the band gap of the DWCBNNT increases with an increase in IWD (decrease in inner tube diameter) and decreases with a decrease in IWD (increase in inner tube diameter). In all three cases, the bands are formed by the molecular orbitals of the armchair CBNNT which are transformed to a series of continuous energy levels; the behaviors of electrons that formed the heterostructure are related to the behavior of electrons in B, C, and N atoms. From the optical properties perspective, the studies were conducted in parallel and perpendicular directions to the nanotubes' axes. The presence of static dielectric functions in parallel direction at 3.3, 3.4, and 4.5 for nanotubes under 3.0 nm, 2.5 nm, and 1.5 nm demonstrated optical refraction. Refractions were also observed in directions perpendicular to the nanotubes. Furthermore, optical reflections occur when there is a higher absorption. The ability of these CBNNT hybrid systems to refract in all directions revealed the most exciting properties of the armchair CBNNT suitable to be used in magnifying glass materials. The findings further imply that the optical absorption coefficient is inversely related to the diameter of the nanotubes and is directly correlated to the band gap.

1. Introduction

Carbon nanotubes (CNTs) are fundamentally exciting materials for solid-state physics because of their novel electronic structure and relatively massless Dirac-fermion characteristics [1]. When two-dimensional (2D) graphene is rolled up into a tubular seamless cylinder, the CNTs are formed with excellent electrical, mechanical, thermal, optical, and magnetic properties [2]. The CNT was discovered in 1991 by Leo and Seo [3], and today they are considered as promising materials for the next-generation optoelectronic devices. On the other hand, boron nitride nanotube (BNNT) is a polymorph of boron nitride (BN) and was predicted in 1994 by Chen et al. [4] and synthesized in 1995 by Li, and since then, BNNT has become one of the most intriguing noncarbon nanotubes. BNNTs are an isomorph of carbon nanotubes (CNTs) with similar structural properties [5], except for a physical difference in terms of their appearance. The CNTs are black while BNNTs are white and sometimes appear as yellow due to the presence of some vacancies by N atoms. However, similar to armchair, zigzag, and chiral CNTs, there are also armchair, zigzag, and chiral BNNTs. Both BNNTs and CNTs are high aspect ratio nano-tubular materials. Studies show that both BNNTs and CNTs are the strongest lightweight nanomaterials with a very high tensile property in the range of Terapascals (TPa). While CNTs are metallic or semiconductors with a narrow bandwidth, the BNNT is a very wide bandgap insulator in the range of 5-6 eV. The electronic band gap of BNNTs is not a function of their chirality and diameter; thus, BNNTs provide good insulation. Furthermore, BN material is an inorganic compound with the chemical formula of BN and is composed of an equal number of nitrogen and boron atoms. It is isoelectronic with a graphene-like structure in which B and N atoms are placed instead of C atoms to form a hexagonal structure like graphite. Boron nitride is soft and a highly resistant material found in various crystalline forms. Also, it has a fixed electronic structure that is formed from a graphite-like boron nitride sheet. BNNTs under the induction of electrons or photons show purple or ultraviolet luminescence while CNTs emit infrared light, and their optical wavelength depends on chirality. Mechanically, both BNNTs and CNTs can be applied as reinforcements, composites, and metal matrix composites [6].

The design and construction of novel materials for superconductivity and high computing resources have been proved possible through the creation of new band gap material by doping a zero band gap material with a wide band gap material. However, the creation process through experimental means is time-consuming, expensive, and tedious. It can also lead to failure due to limited materials. In order to curve this problem, scientists adopt theoretical modeling [6] by appropriately applying computing tools to help narrow down the choices of materials so that the probability of success in experimental work can be achieved. This study fabricates a hybrid hetero combination of (5, 5) SWCNT and (5, 5) SWBNNT, called double-walled carbon boron nitride nanotube (DWCBNNT) and analyzes the electronic and optical properties across different interwall distances (IWDs). It is different from the methods found in literature in which carbon and boron nitride nanotubes were aligned side-by-side known as intertube distance (ITD) as shown in Figure 1. Other works were also done on the CNT/BNNT combinations on the bases of interfacial regions.

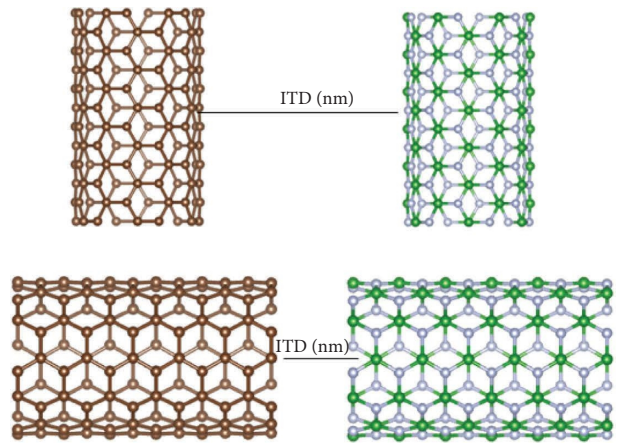

Figure 1: Carbon boron nitride nanotubes showing intertube distance (ITD).

The advantage of adopting the IWD over the ITD is due to the fact that structural defects can easily be detected as a result of new behaviors (such as gas adsorptions) of the nanotubes. Figure 1 presents the diagram of the system under study indicating the IWD; one of the advantages of this method is that symmetry is achieved. The length and chirality of the coupling systems are the same, therefore it is easy to observe an instantaneous change in physical parameters such as a change in shape, size, and volume. A review of the literature shows that only a few studies were performed on the electronic and optical properties of the CBNNT systems under different methods; these are summarized in Table 1.

2. Research Methods

In this research, Kohn-Sham equations were applied by implementing the DFT *ab initio* framework within the Perdiew-Burke-Ernzerhof (PBE) exchange functional. The energy cut-off value for the construction of the plane-wave-based set for DWCBNNT was achieved at 50 Ry, and the k-point value which correlates to the ecut value was $1 \times 1 \times 28$ k-mesh. This gives a total of 28 nk-points in the first Brillouin zone (BZ). The norm-conserving pseudopotentials were used to calculate the ion-electrons attractive interactions. Furthermore, the GW-BSE calculations were performed with the YAMBO code; these were used to calculate the quasi-particle energies and optical properties of the DWCBNNT systems. This is because the GW method provides an accurate description of the electronic structure including quasi-particle corrections [13]. A plane-wave-based set was arranged such that the total energy convergence was 5.5×10^{-6} Ry per carbon atom. In order to avoid intertube interactions, we have created a vacuum from the

Table 1: Status of previous studies in the literature.

Research	Methods	Results and discussion	Remarks	Refs.
Studies of (8, 0) zigzag form of CNT/BNNT	Modes of the CNT/BNNT hetero-junctions were optimized with C-N and C-N interfaces via DFT	Results demonstrated that HOMO-LUMO distributions were based on the CNT section	Failed to explain the effects of the interface separations of C-N and C-B on the electronic properties. Also, it did not report the optical properties	[7]
Study of thermal rectification in carbon/boron nitride heteronanotubes	Studies were performed on the CBNNT interface using nonequilibrium molecular dynamic (NEMD) simulations	Interfacial thermal transport was investigated in which heat flows from BNNT to CNT regions	Did not report the effects of thermal properties on the electronic transport systems of the CBNNT systems	[8]
Electronic transport of zigzag (6, 0) CNT and zigzag (6, 0) BNNT heterostructures	Properties were investigated using first-principle DFT and nonequilibrium green's function formalism for quantum transport calculation	Results revealed that the effects of atomic compositions and joint configuration affect strongly the electronic transport properties	Did not mention anything about the effects of tube length and radius. Also, no information on the optical properties. Besides this, it has been reported that (6, 0) CNT and (6, 0) BNNT cannot exist in nature because two atoms cannot occupy the same lattice space	[9]
Review on carbon and boron nitride nanotubes: structure, property, and fabrications		Reviewed the studies on size, geometry, aspect ratio, chemical composition, and electronic structure that endow them the unique properties. Nanotube basics for CNT and BNNT were covered in this review, such as structures, properties, and synthesis methods	Did not review anything about optical properties. This revealed that a few more investigations are needed for optical properties	[10]
Study the gas sensitivity by the BNNT/SiC hetero combinations	Results were obtained via DFT first principles	A shift in the characteristic vibrational frequency of CO was observed through theoretically computed infrared spectra	There is a need to explore the absorption properties of the BNNT/CNT heterostructures. Also, did not reveal optical properties	[11]
Gas sensing studies of CNT-BNNT-CNT structures	Investigates sensing abilities of NO_2, CO, O_2, and H_2O fluids via first-principle DFT in combination with nonequilibrium green's function formalism	Results revealed higher sensitivity in terms of NO_2 and O_2 and weak sensitivity in terms of H_2O	Reported that CNT-BNNT can adsorb these gases but did not highlight their significant effects on the structural, electronic, and optical properties of the CBNNT system	[12]
Study of the structural, electronic, and optical properties of the armchair CBNNT systems	Studies were performed across various interwall distances (IWD) via DFT *ab initio* with the GW-BSE approach	Results revealed that IWD significantly affects band gap, and optical properties were observed in both parallel and perpendicular directions	It reports higher reflection, refraction, and absorptions in parallel than the perpendicular directions	This work

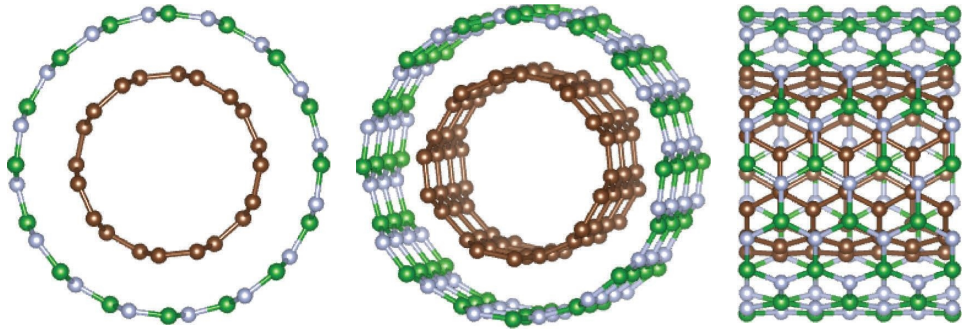

(a) (b) (c)

Figure 2: (a) Top view, (b) slanted view, and (c) side view of armchair CBNNT under 3.0 nm IWD.

optimized lattice parameters concerning the total energy; calculations were performed using a nonspin polarized DFT to save computational cost. To ensure accurate results in this study, the nanotube was appropriately relaxed to proper geometries. The chiral/translation vectors were constructed such that $n = 8$, $m = 8$ for SWBNNT, and $n = m = 6$, 5, and 4 for SWCNT to ensure the proper armchair chirality. The maximum force, stress, and displacements were set at 0.06 eV/Å, 0.06 GPa, and 6×10^{-4} Å, respectively. The unit cell volume is 5515.67 Å^3 with lattice parameters $a = 16.68$ Å and $c = 7.68$ Å. The electronic and optical properties of the DWCBNNT hetero system were studied under 3.0 nm (Figure 2), 2.5 nm (Figure 3), and 1.5 nm (Figure 4) interwall distance. The interwall distance (IWD) is the separation between the wall of the outer SWBNNT and the inner SWCNT structures. It is worth mentioning that to narrow the band gap in the BNNT system, other attempts were performed either by synthetic methods or by arranging the tubes of CNT and BNNT side by side, however, in this work, a new method of intertube coupling has been innovated in which CNTs are coupled to the cylinders of BNNT of relatively larger size to allow for IWD.

3. Results and Discussion

3.1. Structural Optimizations of Armchair DWCBNNT. The scientific properties of the armchair CBNNT are influenced by its mechanical, thermal, and electronic structure. In order to obtain a well-suited heterostructure for this simulation, geometry optimization has been realized. The structure of the hybrid DWCBNNT material was optimized by selecting the nearest neighbor distance of 1.421 Å for carbon atoms and 1.47 Å boron nitride atoms, to ensure accurate calculation with reduced computational cost. The coordinates of the lattice parameter were set as $a_1 = (2.1315,\ 1.23062)$ and $a_2 = (2.1315,\ -1.23062)$. These coordinates help to find the heteronanotube chirality according to the following equation:

$$C = na_1 + ma_2. \quad (1)$$

The chiral translation vectors for a system of the armchair DWCBNNT were, therefore, constructed by

$$C = 5a_1 + 5a_2. \quad (2)$$

The values of n and m shown in the equation in section 2 were used for optimizing the hybrid system of (n, n) CBNNT before relaxation. Table 2 presents the result of the structural optimizations of the DWCBNNT under different IWDs before and after relaxation.

As presented in Table 2, it can be mentioned that there is an inverse variation between the IWD and the diameter of the DWCBNNT system under study which is consistent with other nanotube configurations reported [14]. Also, relaxing the nanotubes does not change the nanotube translation vector because the angle of translation for all armchair nanotubes is 30° irrespective of the size of the nanotube; this also demonstrated that our DWCBNNT system is anisotropic [15].

The first geometric system of the armchair DWCBNNT structure was optimized ensuring 3.0 nm interwall distance (IWD) having the inner tube diameter of 6.89 Å. The (7, 7) armchair SWCNT was coupled with the (8, 8) armchair SWBNNT, and the result obtained was the armchair double-walled CBNNT heterostructure (DWCBNNT). Other two configurations of the armchair DWCBNNT were obtained via the same procedure, and the nanotube with 2.50 nm IWD was obtained by coupling (6, 6) SWCNT with (8, 8) SWBNNT; likewise, the nanotubes under 1.50 nm IWD were obtained by coupling (5, 5) SWCNT with (8, 8) SWBNNT; these are presented in Figures 2–4.

3.2. Electronic Transport of DWCBNNT. To demonstrate the band structure of the hybrid armchair DWCBNNT system, the Fermi energy level was chosen at the zero gamma point. All three systems are semiconductors having a direct band gap at the first Brillouin zone (BZ) [16]. The band structure of armchair CBNNT heteronanotubes was studied under three different IWD of 1.5 nm, 2.3 nm, and 3.1 nm; the results are presented in Figures 5–7. The effects of IWD open up a pseudogap of considerable eV by narrowing the band gap of SWBNNT by SWCNT [16]. As presented in Figure 5(a), a semiconducting property can be observed in the armchair CBNNT hetero nanotube with 3.0 nm IWD. The band gap obtained here is 3.30 eV under KS-DFT while 3.1 eV was obtained for the same structure with G_0W_0quasi-

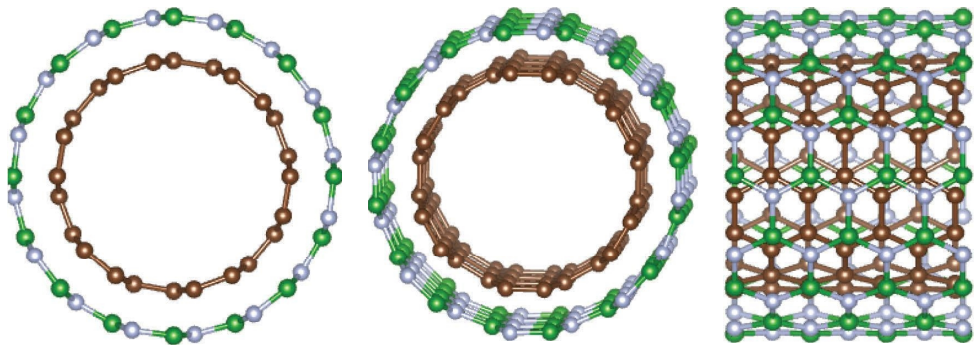

(a) (b) (c)

Figure 3: (a) Top view, (b) slanted view, and (c) side view of the armchair CBNNT under 2.50 nm IWD.

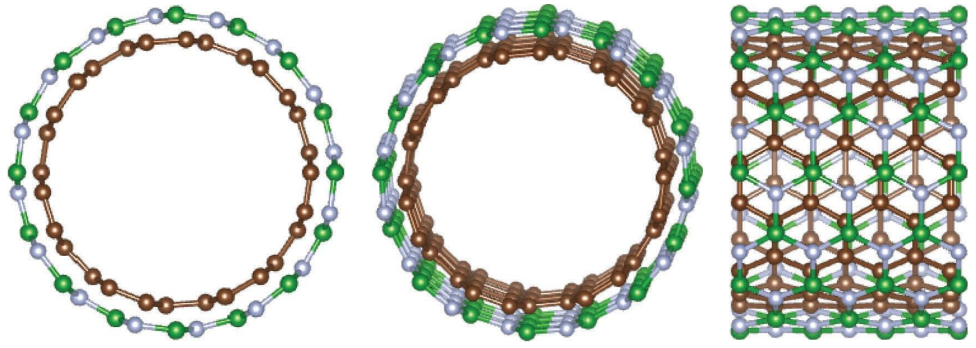

(a) (b) (c)

Figure 4: (a) Top view, (b) slanted view, and (c) side view of armchair CBNNT under 1.50 nm IWD.

Table 2: DWCBNNT before and after relaxation.

IWD (nm)	Diameter (Å)	Chiral vector	Translation vector
Before relaxation			
3.00	9.56	34.10	2.46
2.50	8.15	25.58	2.46
1.50	6.85	21.32	2.46
After relaxation			
3.00	9.58	34.17	2.46
2.50	8.19	25.68	2.46
1.50	6.89	21.42	2.46

particle corrections which is blue-shifted. This result is consistent with the characteristics of G_0W_0 calculations, i.e., yielding small band gaps [17]. The corresponding density of states is presented in Figure 6(b). The effects of IWD can be easily observed by comparing the bands' structure of Figure 5(a) with Figures 6(a) and 7(a), and the corresponding density of states is shown in Figures 6(b) and 7(b). At the equilibrium gamma points, no bands are seen crossing the Fermi level or intersections at the Dirac point as such all the structures can be regarded as semiconductors [18]. For the case of armchair CBNNT calculated with 2.30 nm IWD, results are shown in Figure 6(a). There is a relatively narrow band gap than the results obtained in Figure 5(a). The energy states were seen a bit far from the Fermi level due to the decrease of IWD from 3.0 nm to 2.30 nm. This resulted in the creation of a narrow band gap of 1.79 eV (1.8 eV with G_0W_0). A narrower band gap of 0.81 eV (1.01 eV with G_0W_0) was obtained when the IWD is further reduced to 1.50 nm as shown in Figure 7(a). This indicates that shorter IWD encourages more interaction between carbon atoms towards narrowing the band gap of the armchair CBNNT system [19]. Just like carbon nanotubes, diameters of armchair CBNNTs can be obtained by

$$d = \frac{a}{\pi}\sqrt{n^2 + nm + m^2}, \tag{3}$$

where a is the lattice constant in armchair CBNNT. The results of the effects of IWD on the electronic band gaps are shown in Table 3.

As presented in Table 3, it is evident that increasing the IWD widens the band gap up to some limits before the breaking of the bond. In all three cases, the bands are formed by the molecular orbitals of the armchair CBNNT which are transformed to a series of continuous energy levels [20], and the behaviors of electrons that formed the heterostructure are related to the behavior of electrons in B, C, and N atoms. Bands are formed in Figures 5, 6(a), and 7(a) because the discrete energy levels are perturbed through the quantum mechanical effects of IWD and the occupation of the valence bands by many electrons. As observed in Figures 5(a) and 6(a), the highest energy in the valence band and at the same magnitude as the lowest energy in the conduction band are

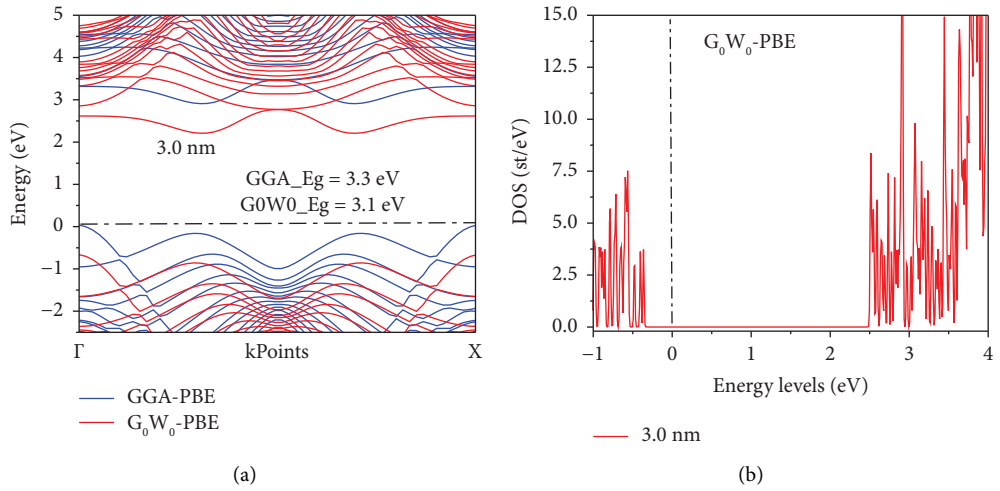

Figure 5: (a) Bands structure and (b) electronic density of states for CBNNT with 3.0 nm IWD.

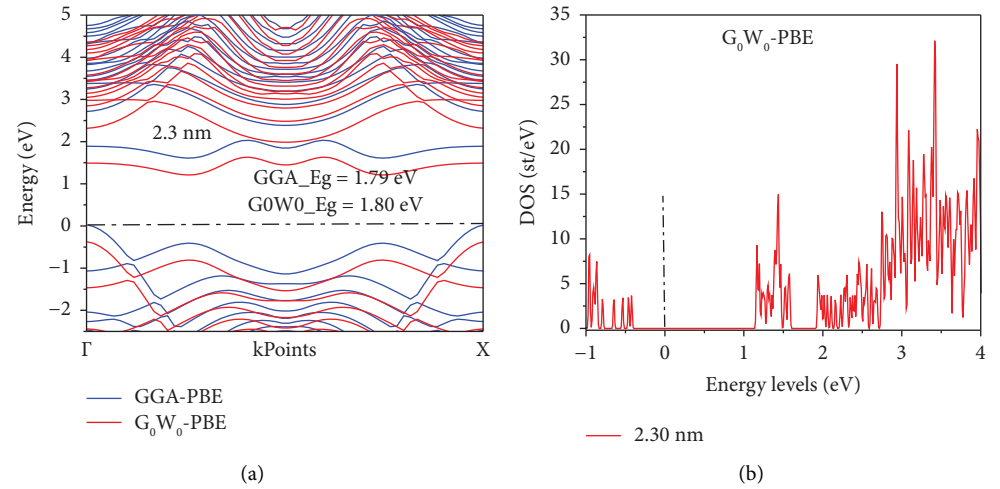

Figure 6: (a) Bands structure and (b) electronic density of states for CBNNT with 2.30 nm IWD.

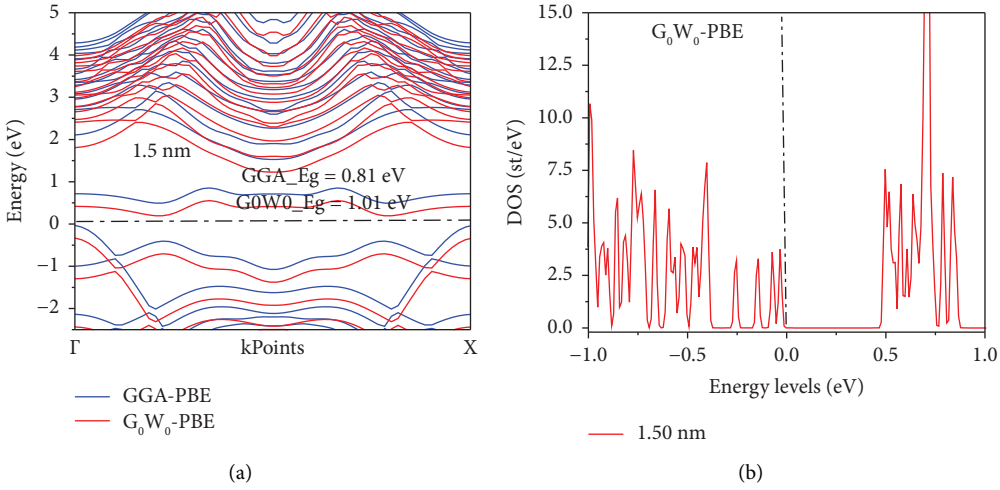

Figure 7: (a) Bands structure and (b) electronic density of states for CBNNT with 1.50 nm IWD.

Table 3: Effects of IWD on the electronic properties of DWCBNNT.

Structure	IWD (nm)	Inner diameter (Å)	DFT bandgap (eV)	G_0 W_0 bandgap (eV)
CBNNT	3.00	7.10	3.30	3.10
CBNNT	2.30	7.60	1.79	1.80
CBNNT	1.50	8.00	08.1	1.01

thus at the same momentum which allows the recombination of holes and electrons when the transition takes place. As such a direct band gap [21] is formed, momentum is conserved and energy is released in the form of light.

The quasi-particle band gaps are formed from the weak interactions of SWCNT and SWBNNT atoms which are renormalized to smaller values in the presence of dielectric substrates of boron nitride nanotubes [22]. The narrowing of the band gap is due to the polarization-induced screening effects which change the correlation energy of the SWCNT orbitals which stabilizes the valence band [23]. To further confirm the electronic properties obtained from pseudo-calculations presented above, we have carried out studies of the number of occupations by electrons that take part in the interaction process. The studies of the electronic density of states (DOS) help us to understand more about the energy level distributions that can be occupied by electrons in the quasi-particlehetero-structure. This is achieved by revealing the number of different states in the particular energy level allowed to be occupied by excitons.

Figures 5(b), 6(b), and 7(b) demonstrate the total density of states for the CBNNT systems under IWD of 30 nm, 2.30 nm, and 1.50 nm, respectively with the G_0W_0 method. All the figures reported zero DOS at the Fermi energy level which confirmed the semiconducting properties of the hybridized armchair CBNNT system. As presented in Figure 6(b), the energy states were seen a bit far from the Fermi level due to a decrease of IWD from 3.0 nm to 2.30 nm. This results in the creation of a narrow band gap of 1.80 eV. More bands are seen in the conduction band than in the valence band because of the screened excitation by P′ orbitals of the C atom. Similarly, a band gap of 1.01 eV was obtained in the case of 1.5 nm as shown in Figure 7(b). Based on the results obtained, our computational results revealed that increasing the IWD widens the band gap of the system of the armchair CBNNT heteronanotubes [24]. The results obtained are consistent with the previous ones obtained by other methods [25]. Therefore, by examining the band structure and the density of states, we can mention that as the IWD of the armchair CBNNT increases, the band gap increases while the DOS decreases [26].

3.3. Optical Properties of the Armchair DWCBNNT. In order to understand the precise properties of low dimensional materials that will make them suitable for next-generation nanoscience and technology, it is necessary to figure out its response to interactions with incident electromagnetic energy; this is called photon energy [27]. When an incident light impinges on a material, some of it is refracted, some are absorbed, and some are transmitted and so on depending on the nature of the material. The number of incident photons refracted, transmitted, absorbed, reflected, or conducted by a material reveals its suitable area of application. The study of the optical properties of solids is essential for analyzing their atomic and electronic structure. In this research, optical properties in terms of electron-electron interactions are studied using the random phase approximation (RPA); this deals with the real and imaginary parts of the dielectric function, refractive index, extinction coefficient, electron energy loss function, optical absorption, and optical conductivity. Nanotube structures exhibit different responses to electromagnetic radiation in different directions.

3.3.1. Complex Dielectric Functions. We use the complex dielectric functions to report the optical properties of the hybrid armchair CBNNT systems under different IWDs. This is achieved through the description of the nanotube response from the incident electromagnetic fields which in turn is a function of the band structure of the CBNNT systems. Full descriptions of the real and imaginary dielectric constants for the armchair CBNNT heterosystem are presented in Figures 8 and 9. The studies were conducted for the incident photon in both parallel (z-direction) and perpendicular (x-direction) to the nanotube axis. Figure 8 presents the real spectrum of the dielectric function; as can be seen, the presence of peaks was observed along the nanotubes at 3.5, 3.5, and 4.5 for 3.0 nm (Figure 8(a)), 2.30 nm (Figure 8(b)), and 1.50 nm (Figure 7(c)), respectively. Lower peaks can also be observed in the perpendicular direction of all three nanotube configurations. The presence of these peaks confirms the dielectric functions; similarly, the presence of peaks in both parallel and perpendicular directions demonstrates that our CBNNT systems respond to electromagnetic waves in all directions.

From the diagram of the imaginary dielectric functions presented in Figure 9, under 3.0 nm IWD, a bound state can be observed at 3.2 eV and 3.3 eV in parallel and perpendicular directions, respectively. This is the threshold for the optical and band gap for this nanotube. Furthermore, the values agreed well with the band gap obtained under 3.0 nm IWD (see Figure 2); this further confirmed our earlier claim that the nanotube response incident electromagnetic fields are a function of the band structure. Other bound states obtained are 1.6 eV and 0.9 eV under 2.30 nm and 1.50 nm, respectively. These are shown in Figures 9(b) and 9(c), respectively. The optical absorption edges can be confirmed by the presence of the raise in the peaks below 5 eV in the imaginary dielectric and as well as constant behavior above 15 eV. In the parallel directions, three peaks were observed in Figure 9(b) under 2.30 IWD; similarly, two other peaks were observed in Figure 9(c). These are due to the intraband transitions (absorption by free electrons). When compared

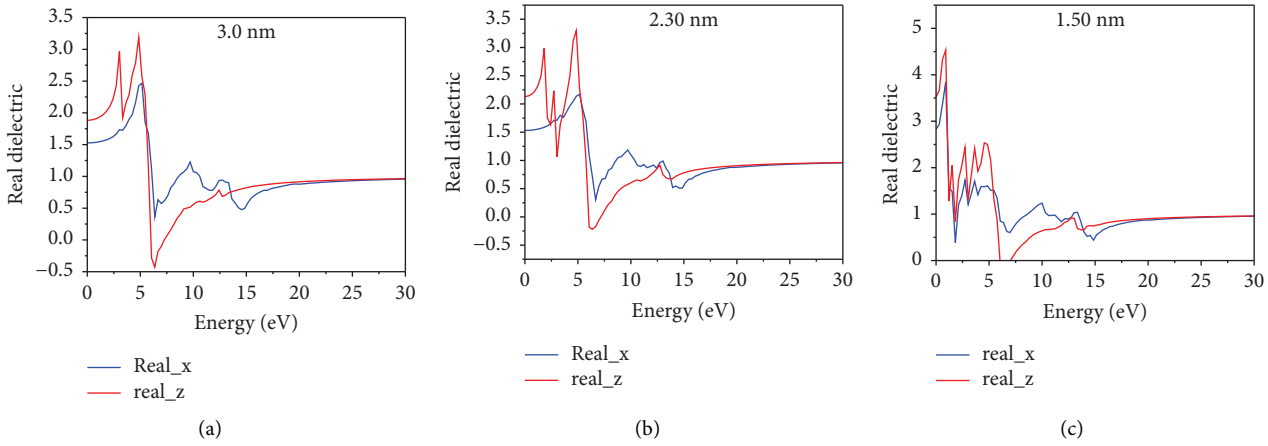

Figure 8: Real dielectric functions for armchair CBNNT under different IWDs.

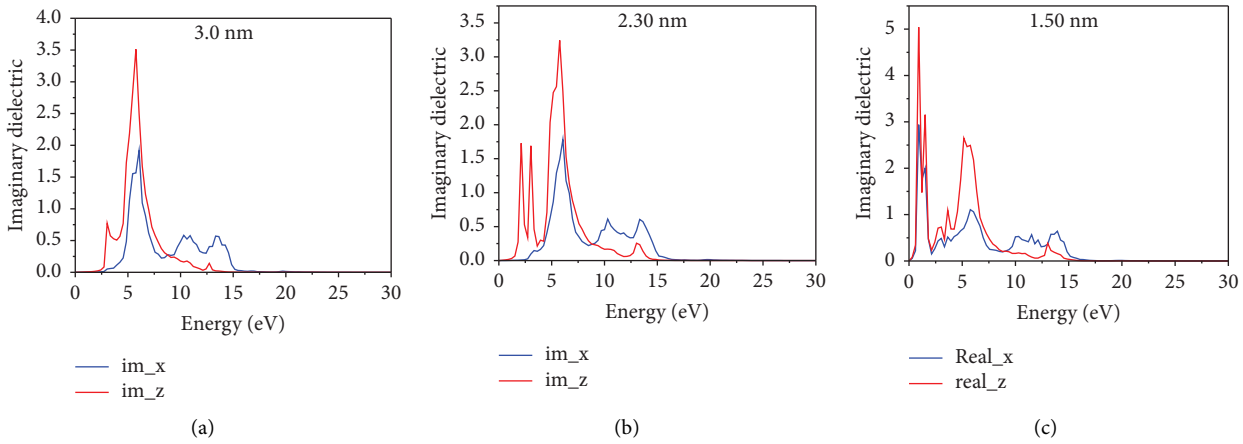

Figure 9: Imaginary dielectric functions for armchair CBNNT under different IWDs.

under different IWDs, it can be reported that the higher dielectric function is observed for 1.50 nm which has the smallest IWD and larger diameter, as such dielectric function is inversely related to the diameter of the nanotube. There are also direction variations between the dielectric functions and the intensity of the band gap. Furthermore, the imaginary dielectric function is partly the result of the actual transfers between occupied and unoccupied states. It can also be reported that the interband transition is because of the excitations at the absorption edges. Also, absorptions are higher in the parallel than perpendicular direction for all the nanotube configurations.

3.3.2. Electron Energy Loss. The calculated energy loss function was presented in order to further study the energy released by an electron upon exiting another band. The results were shown in Figure 9; different photons combined to excite with different frequencies. This may further help us to understand the absorption peaks in both systems of our CBNNT nanotubes. There is a greater loss of energy in the parallel direction; this can be justified by the peaks at the intensity of 1.9 (Figure 10(a)), 1.89 (Figure 10(b)), and 1.99 (Figure 10(c)). Virtually, the amount of energy loss under 3.0 nm, 2.30 nm, and 1.50 nm is approximately the same. This amount of energy loss is due to the high interactions of photons with electromagnetic radiation. Smaller π-electronic peaks were also seen in all cases of perpendicular to the tube axis with predominantly higher Plasmon peaks in the parallel directions. However, more energy is lost in the perpendicular direction, hence less absorption.

3.3.3. Optical Refraction and Extinction. As per the literature, the refraction properties of nanomaterials are analyzed in terms of the crystallographic structure and velocity of the incident photon. We define the static refractive index as the value of the index of refraction at zero energy level [27]. This value of the static refractive index is equal in magnitude to the value of the static dielectric constant [28]. In this study, we report the static refractive indices of the armchair CBNNT under 3.0 nm, 2.50 nm, and 1.50 nm IWD; results so far obtained are presented in Figure 11. For all three configurations, the refractive index reaches a minimum value between 7 and 8 eV; the refraction also becomes constant from 17.5 eV. Therefore, reflection is increased in these regions; refractions are also recorded in both directions. Therefore, all three systems can be regarded as transparent.

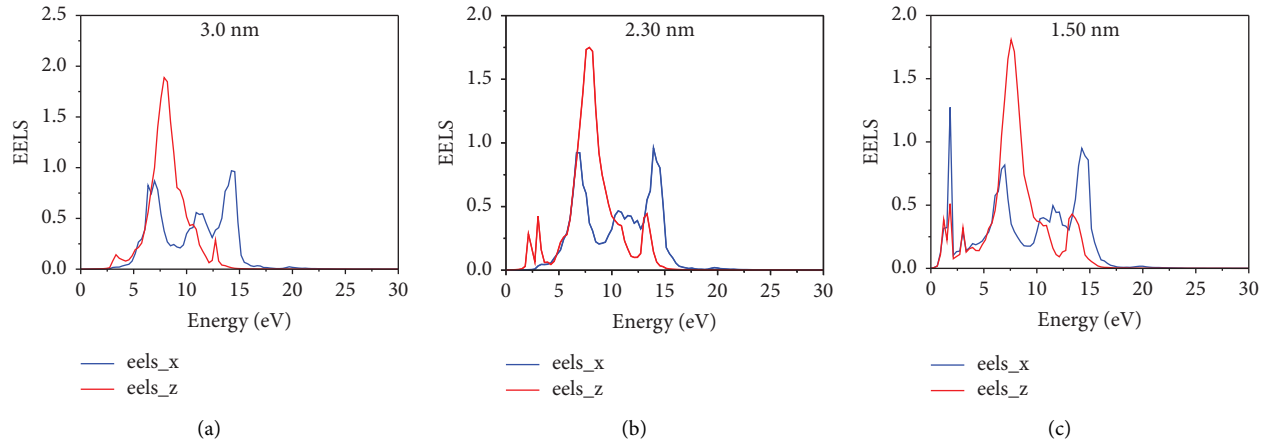

Figure 10: Electron energy loss spectrum for armchair CBNNT under different IWDs.

However, the systems in Figures 11(a) and 11(b) demonstrate lower refraction than the system in Figure 11(c); therefore, CBNNT under 1.50 nm is regarded as more transparent. Furthermore, it can be inferred that the optical refractive index is a function of the real dielectric constant based on the similarities with static dielectric values. The ability of this hybrid system of the CBNNT to refract in all directions revealed the most exciting properties of the armchair CBNNT to be applied for use in magnifying glass materials [29]. The lowest refractions are recorded in both systems; also, the refraction becomes generally constant from 15 eV, as such the CBNNT demonstrates low refraction generally in the visible range. Furthermore, the refractive index decreases with the increase in incident photon energy after 5 eV; here, the phase velocity of the passing light is higher than the speed of light in a vacuum; this behavior is called normal dispersion [30]. This provides the photoluminescence phenomenon in CBNNT.

The coefficient of extinction in Figure 12 similarly shows that there is a gap in both directions of the incident light, and the peaks are in the range of 7 eV. In this energy range, there is a maximum drop in the amplitude of the incident wave for hybrid CBNNT. While a more uniform behavior is seen in perpendicular directions, the amplitudes of the electromagnetic waves are higher in parallel than in perpendicular directions.

As presented in Figures 12(a) and 12(b), the higher transmission of a photon is seen in direction parallel to the nanotube axis; meanwhile, more peaks appeared in the system of Figure 12(c) which demonstrates more transmissions. The coefficient of extinction for CBNNT was seen to be in one region only (Figure 12(a)); however, after increasing the IWD, many peaks appeared (Figure 12(c)). There are also transmissions in perpendicular directions. From our results, it can be reported that CBNNT transmits photons in all directions. Because of the effects of IWD, the system in Figure 12(c) has higher transmission than the system in Figure 12(a). The transmission properties of this new system of CBNNT bring it to use as sensors for mobile phone touch screens [31]; also, the transmission has increased from ultraviolet to the visible range region.

3.3.4. Reflection. The spectrum of optical reflection for the armchair CBNNT under different IWDs is presented in Figure 13. According to this spectrum, armchair CBNNT generally demonstrated lower reflection than refraction. As can be seen, the highest intensity of the reflection is 0.25 (Figure 13(a)) as compared to the highest refraction peak of 2.4 in Figure 13(c). Maximum reflection was observed at the energies in which the highest absorption occurs. For example, the maximum reflection under 3.0 nm in the parallel direction is 2.12 at 5 eV; this corresponds to maximum absorption of $20 \times 10^{-8}\,\mathrm{cm}^{-1}$ in the absorption spectrum of Figure 14(a). Lower reflections observed in the perpendicular directions to the nanotube axes demonstrated the nanotubes' high aspect ratio. Generally, decrease in the IWD increases reflection peaks, for example, in Figure 13(a), smooth peaks are seen for CBNNT under 3.0 nm; as the IWD is further decreased to 2.30 nm (increase in the tube diameter), more peaks appear as shown in Figure 13(b). Further increases in reflection peaks are observed in Figure 13(c) due to a further decrease in the IWD to 1.50 nm. This means that the reflection coefficient has an inverse relation with the nanotubes' diameter and is directly related to the IWD. The rise and fall in the reflection peaks in the energy range from 2.7 eV to 17 eV which demonstrate the CBNNT's ability to serve as a potential candidate for the next generations' optoelectronic chips. Furthermore, the reflection occurs in the range of ultraviolet region which suggests its potential for quality control in the beverage industry and chemical research.

3.3.5. Optical Absorption. The absorption spectrum of armchair DWCBNNT under different IWDs is shown in Figure 14. From the figure, the allowable optical transitions of the electron between the empty states of the conduction band and the filled states of the valence band were observed. The threshold energy for the transition in the absorption spectrum corresponds to the gap size in the band structure of CBNNT nanotubes, and it means that the electrons are excited and make a transition by getting the lowest energy that is larger than the band gap value. The comparison

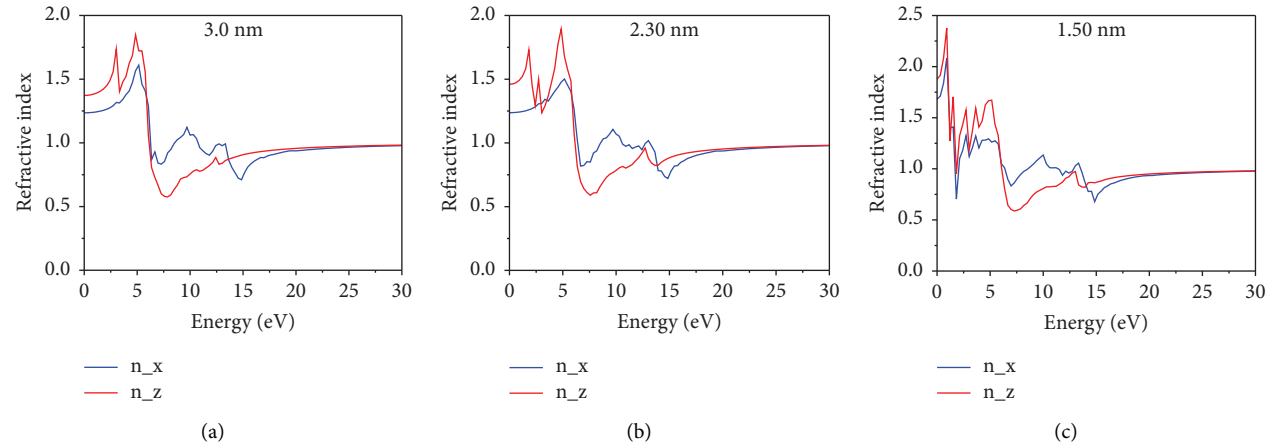

Figure 11: Refractive indices for armchair CBNNT under different IWDs.

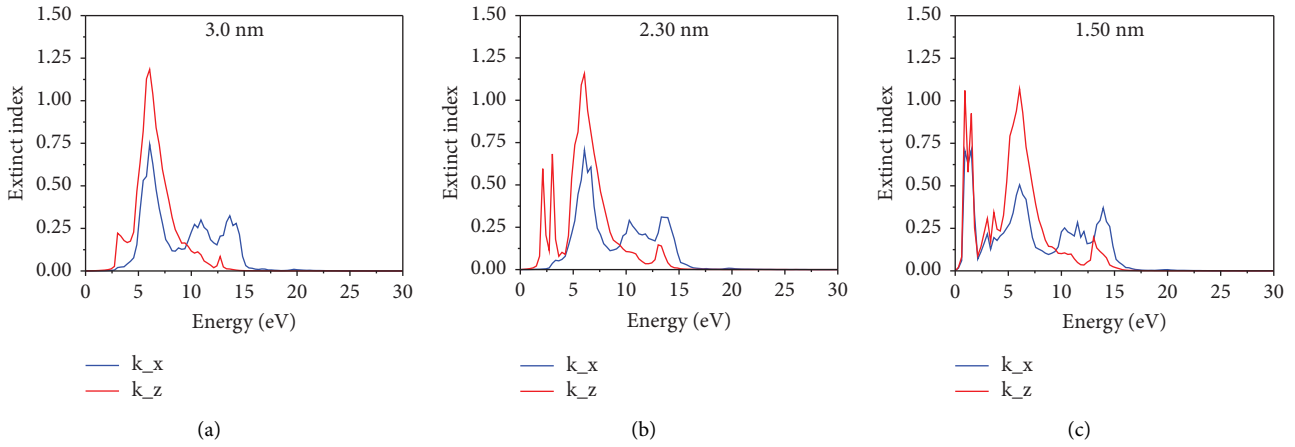

Figure 12: Extinct indices for armchair CBNNT under different IWDs.

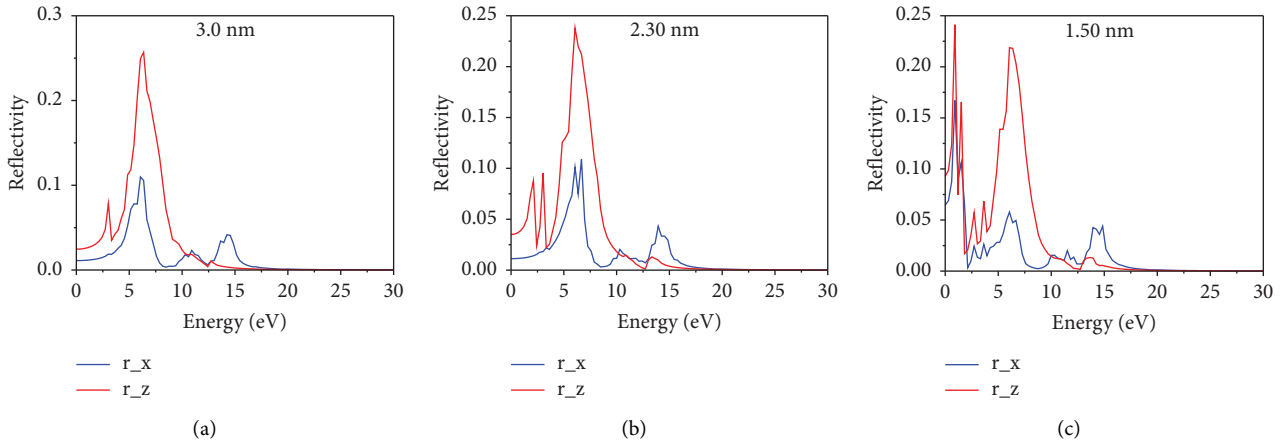

Figure 13: Optical reflectivity for armchair CBNNT under different IWDs.

between different nanotubes with various diameters also indicates that the highest absorption is associated with the armchair DWCBNNT nanotube under 3.0 nm (Figure 14(a)) which has the smallest diameter and largest gap, and the lowest absorption is correlated to the armchair DWCBNNT nanotube which has the largest diameter and the smallest

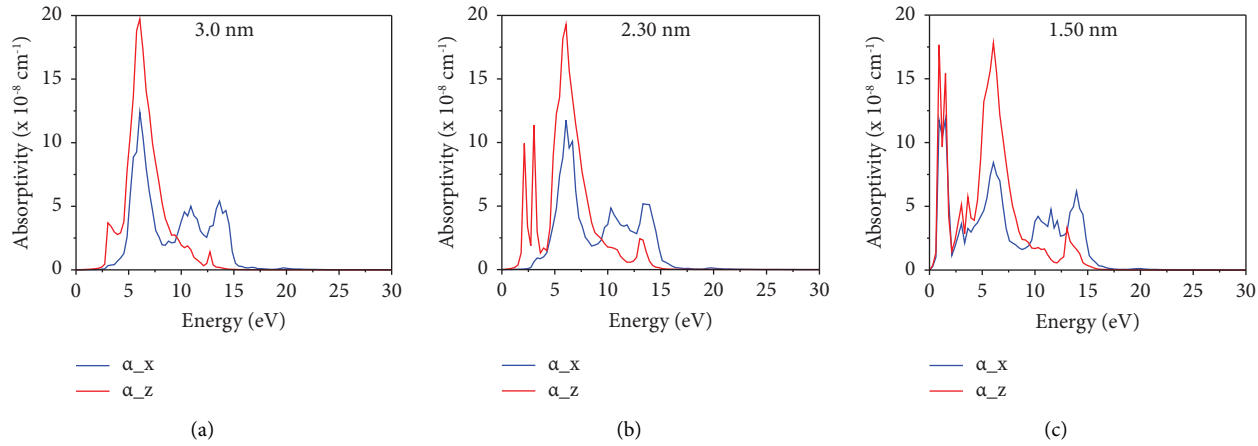

Figure 14: Optical absorptions for armchair CBNNT under different IWDs.

gap (Figure 14(c)). These findings imply that the optical absorption coefficient is inversely relevant to the diameter of the nanotubes and is directly correlated to the band gap.

4. Conclusions

In conclusion, we have performed DFT calculations on the hybrid DWCBNNT heteronanotube under different IWDs. Due to the effects of IWD, new features were observed in the DWCBNNT system which makes it as a potential material for advanced applications. Calculations of the electronic band structure revealed that the band gap varies directly with the IDW and inversely with the inner tube diameter, for example, a band gap of 3.3 eV (KS-DFT) was obtained under 3.0 nm and 0.81 eV (KS-DFT) was obtained under 1.5 nm. Results from quasi-particle corrections with a one-shotG_0W_0 method indicated a blue shift under 3.0 nm and a red shift with 2.3 nm and 1.5 nm, respectively. In all three cases, the bands are formed by the molecular orbitals of the armchair CBNNT which are transformed into a series of continuous energy levels. The behaviors of electrons that formed the hetero-structure are related to the behavior of electrons in B, C, and N atoms because the discrete energy levels are perturbed through quantum mechanical effects of IWD and the occupation of the valence bands by many electrons. Moreover, the studies were conducted for the incident photon in directions both parallel (z-direction) and perpendicular (x-direction) to the nanotube axis. The presence of peaks in both parallel and perpendicular directions demonstrates that our CBNNT systems respond to electromagnetic waves in all directions. Virtually, the amount of energy loss under 3.0 nm, 2.30 nm, and 1.50 nm are approximately the same, which is due to the high interactions of photons with electromagnetic radiations. Generally, the rise and fall in the absorption peaks, higher refractions, and reflections behavior reveal the potential of this material to serve as the next generation's optoelectronic devices.

Data Availability

All data used to support the findings of the study are included within the manuscript.

Conflicts of Interest

The authors declare that they have no conflicts of interest.

Authors' Contributions

Y.S.I. and A.B.S. conceptualized the study; Y.S.I., I.I.I., and C.E.N. proposed the methodology; Y.S.I., C.E.N., R.R., and A.L. provided the software; Y.S.I., I.I.I., and A.B.S. performed formal analysis; S.M.E., A.A.M., and I.K. provided the resources; M.U.K. and Y.S.I. curated the data; Y.S.I. prepared the original draft; M.U.K. reviewed and edited; M.R.I.F. and I.K visualised the manuscript. All authors have read and agreed to the published version of the manuscript.

Acknowledgments

The authors also acknowledge Federal University Dutse-Nigeria, for giving resource training to the lead researcher, Bauchi State University Gadau-Nigeria, and the Tertiary Education Trust Fund (TETFund)-Nigeria for providing resources, funds, and avenue for the successful conduct of this research.

References

[1] J. S. Ponraj, Z. Q. Xu, S. C. Dhanabalan et al., "Photonics and optoelectronics of two-dimensional materials beyond graphene," *Nanotechnology*, vol. 27, no. 46, Article ID 462001, 2016.

[2] A. Szentes, C. Varga, G. Horvath et al., "Electrical resistivity and thermal properties of compatibilized multi-walled carbon nanotube/polypropylene composites," *Express Polymer Letters*, vol. 6, no. 6, pp. 494–502, 2012.

[3] D. W. Lee and J. W. Seo, *Preparation of Carbon Nanotubess from Graphite Powder at Room Temperature*, Cambridge University, Cambridge, UK, 2014.

[4] X. Chen, P. Wu, M. Rousseas et al., "Boron nitride nanotubes are noncytotoxic and can Be functionalized for interaction with proteins and cells," *Journal of the American Chemical Society*, vol. 131, no. 3, pp. 890-891, 2009.

[5] Y. Li, "Boron-nitride nanotube triggered self-assembly of hexagonal boron-nitride nanostructure," *Physical Chemistry Chemical Physics*, vol. 16, no. 38, pp. 20689–20696, 2014.

[6] A. J. Ferdaus, K. U. Mayeen, H. M. Mahadi, and Y. S. Itas, "Cancerous and non-cancerous brain MRI classification method based on convolutional neural network and log-polar transformation," *Healthcare*, vol. 19, no. 9, p. 1094, 2022.

[7] M. K. Mahata, S. Ghosh, S. Das, and D. Biswas, "Universal band gap DeterminationModel for doped semiconductor materials," *ECS Solid State Letters*, vol. 4, no. 12, pp. P98–P101, September 2015.

[8] L. Hongxia, Z. Heming, S. Jiuxu, and Z. Zhiyong, "Electronic structures of an (8, 0) boron nitride/carbon nanotube heterojunction," *Journal of Semiconductors*, vol. 31, no. 1, Article ID 013001, 2010.

[9] X. K. Chen, Z. X. Xie, Y. Zhang et al., "Highly efficient thermal rectification in carbon/boron nitride heteronanotubes," *Carbon*, vol. 148, pp. 532–539, 2019.

[10] P. Zhao, D. Liu, Y. Zhang et al., "Electronic transport properties of zigzag carbon- and boron-nitride-nanotube heterostructures," *Solid State Communications*, vol. 152, no. 12, pp. 1061–1066, 2012.

[11] L. Chang and F. Qichen, "Carbon and boron nitride nanotubes: structure, property and fabrication," *ES Materials and Manufacturing*, vol. 3, pp. 2–15, 2019.

[12] Shreyas, "Comparative study on adsorption behaviour of the monolayer graphene, boron nitride and silicon carbide hetero-sheets towards carbon monoxide: insights from first-principle studies," *Computational and Theoretical Chemistry*, vol. 1211, 2022.

[13] S. S. Vedaei and E. Nadimi, "Gas sensing properties of CNT-BNNT-CNT nanostructures: a first principles study," *Applied Surface Science*, vol. 470, pp. 933–942, 2019.

[14] M. E. Foster and B. M. Wong, "Nonempirically tuned range-separated DFT accurately predicts both fundamental and excitation gaps in DNA and RNA nucleobases," *Journal of Chemical Theory and Computation*, vol. 8, no. 8, pp. 2682–2687, 2012.

[15] Y. S. Itas, A. B. Suleiman, C. E. Ndikilar et al., "Computational studies of the excitonic and optical properties of armchair SWCNT and SWBNNT for optoelectronics applications," *Crystals*, vol. 12, no. 6, p. 870, 2022.

[16] Y. S. Itas, A. B. Suleiman, C. E. Ndikilar et al., "The exchange-correlation effects on the electronic bands of hybrid armchair single-walled carbon boron nitride nanostructure," *Crystals*, vol. 12, no. 3, p. 394, 2022.

[17] S. Aminu Yamusa, A. Shaari, I. Isah et al., "Effects of exchange correlation functional (Vwdf3) on the structural, elastic, and electronic properties of transition metal dichalogenides," *Journal of the Nigerian Society of Physical Sciences*, vol. 5, no. 1, p. 1094, 2023.

[18] K. Young, "Effect of intertube coupling on the electronic structure of carbon nanotube ropes," *Physical Review B*, vol. 58, no. 20, 2016.

[19] M. Shishkin and G. Kresse, "Self-consistentGWcalculations for semiconductors and insulators," *Physical Review B*, vol. 75, no. 23, Article ID 235102, 2007.

[20] Alexander, "Electrochemical view of the band gap of liquid water for any solution," *World Journal of Condensed Matter Physics*, vol. 4, no. 4, pp. 1–6, 2014.

[21] M. Li and J. Li, "Size effects on the band-gap of semiconductor compounds," *Materials Letters*, vol. 60, no. 20, pp. 2526–2529, 2006.

[22] Y. S. Itas, A. B. Suleiman, A. S. Yamusa, R. Razali, and A. M. Danmadami, "Ab'initio studies of the structural and electronic properties for single-walled armchair MgONT, SiCNTs and ZnONTs for next generations' optoelectronics," *Gadau Journal of Pure and Allied Sciences*, vol. 1, no. 2, pp. 160–165, 2022.

[23] N. A. Lanzillo, N. Kharche, and S. K. Nayak, "ERRATUM: substrate-induced band gap renormalization in semiconducting carbon nanotubes," *Scientific Reports*, vol. 4, no. 1, p. 4317, 2014.

[24] Y. S. Itas, C. E. Ndikilar, and T. Zangina, "Carbon nanotubes: a review of synthesis and characterization methods/techniques," *The International Journal of Science & Technoledge*, vol. 8, no. 2, pp. 43–50, 2020.

[25] M. Tyunina, L. Yao, D. Chvostova et al., "Concurrent bandgap narrowing and polarization enhancement in epitaxial ferroelectric nanofilms," *Science and Technology of Advanced Materials*, vol. 16, no. 2, Article ID 026002, 2015.

[26] S. Inoue, H. Suto, W. Wongwiriyapan, T. Kimura, Y. Murata, and S. M. Honda, "Density of states of single-walled carbon nanotubes grown on metal tip apex," *Applied Physics Express*, vol. 2, no. 3, pp. 035005–35013, 2009.

[27] J. A. Talla, "Stability and electronic properties of hybrid coaxial carbon nanotubes–boron nitride nanotubes under the influence of electric field," *Applied Physics A*, vol. 127, no. 8, p. 628, 2021.

[28] N. Louis et al., "Band structure, density of states and superconductivity of adsorbed titanium chains on (8,8) and (14,0) carbon nanotubes," *Materials Physics and Mechanics*, vol. 10, pp. 72–81, 2010.

[29] Y. S. Itas, A. B. Suleiman, C. E. Ndikilar et al., "DFT studies of structural, electronic and optical properties of (5, 5) armchair magnesium oxide nanotubes (MgONTs)," *Physica E: Low-Dimensional Systems and Nanostructures*, vol. 149, Article ID 115657, 2023.

[30] Y. S. Itas, C. E. Ndikilar, T. Zangina et al., "Synthesis of thermally stable h-BN-CNT hetero-structures via microwave heating of ethylene under nickel, iron, and silver catalysts," *Crystals*, vol. 11, no. 9, p. 1097, 2021.

[31] Y. Saadu Itas, A. B. Suleiman, C. E. Ndikilar et al., "Effects of oxygen absorption on the electronic and optical properties of armchair and zigzag Silicon Carbide Nanotubes (SiCNTs)," *Physica Scripta*, vol. 98, no. 1, Article ID 015824, 2022.